1997

Liquid-Liquid Phase Separation in Multicomponent Polymer Systems

William MacKnight, *University of Massachusetts Amherst*
Ronald Koningsveld

LIQUID-LIQUID PHASE SEPARATION

IN MULTICOMPONENT POLYMER SYSTEMS

XXVII. Determination of the pair-interaction function for polymer blends*

Ronald Koningsveld and William J. MacKnight

Sylvio O. Conte National Center for Polymer Research,
University of Massachusetts, Amherst, MA 01003, USA

Dedicated to Professor Bob Stepto (UMIST, Manchester, UK)
on the occasion of his 60th birthday

Abstract

It is demonstrated that estimation of the pair-interaction function from polymer-blend cloud points cannot yield meaningful values if data are restricted to a single blend. Additional information is required, such as cloud points in another blend made up of samples of the same two polymers differing in molar mass or, alternatively, scattering data on the original blend. Information obtained from melting points of a crystallizable constituent in the blend is insignificant in this respect. Molar-mass distributions in the constituents of the blend complicate the analysis, and must be known in considerable detail.

Introduction

The molecular heterogeneity occurring in virtually all synthetic polymers poses problems when mixtures of such materials are subjected to a thermodynamic analysis by means of the pair-interaction parameter. This parameter, usually denoted by χ, depends at least on temperature and concentration, and knowledge of this dependence permits predictions of equilibrium liquid-liquid phase behaviour of the blend. It is practically impossible to extract meaningful values for the interaction function from a single measured cloud-point curve (temperature of incipient turbidity against blend composition) and additional data cannot be dispensed with, even when the molecular heterogeneity is negligibly small. The analysis is further complicated by the presence of molar-mass distributions (*mmd*) which cause the two cloud-point concentrations at a given temperature not to represent coexisting phases, as they do in the strictly-binary case[1-3].

The present paper demonstrates that the extraction of useful values for the interaction function from a measured cloud-point curve (*cpc*) not only requires quite accurate knowledge of the *mmd*'s involved but still needs additional

* Part XXVI: ref. 33.

information. Such extra data may either be cloud points in a blend of samples with different *mmd*'s, or spinodal scattering data on the original blend. We illustrate this statement with examples of partial-miscibility behaviour and of measurements of melting-point depression, discussing

(*a*) experimental cloud points in the system polyisoprene/polystyrene, in which both constituents have a very narrow *mmd*. The *mmd*'s can be ignored for the present practical purpose, and such systems have therefore been termed *practically*-binary[4]. The analysis reveals some of the subtleties adherent to polymer/polymer miscibility, and their incorporation into suitable models[5,6];

(*b*) the effect of *mmd*'s on the extraction of significant χ values which is investigated with the aid of calculated *cpc*'s for well-defined *mmd*'s. We employ Flory-Huggins-Staverman (*FHS*) thermodynamics[7-13] in which χ depends solely on temperature, and show in passing that a possible concentration dependence of χ does not alter the problem essentially. Having fixed the two *mmd*'s and the temperature dependence of χ we have *a priori* knowledge on each of the two features that determine the *cpc*, *i.e.*, the *mmd*'s and $\chi(T)$;

(*c*) the insensitivity of melting points in partially crystallizable blends to essential details of the interaction function.

Practically-binary blends

Assuming the residual polydispersity in narrow-distribution polymer samples to be negligible, we may apply the strictly-binary version of the *FHS* expression for the free enthalpy (Gibbs free energy) of mixing, ΔG,

$$\Delta G/NRT = \Omega_1 + \Omega_2 + g(T,\varphi_2)\varphi_1\varphi_2 \qquad (1)$$

where φ_k is the volume fraction of component k, the last term on the r.h.s. is the familiar Van-Laar interaction function, and $\Omega_k = (\varphi_k/m_k)ln\varphi_k$ (k = 1,2). The system is thought to be built up of N identical basic volume units (*BVU*), and m_k is the number of *BVU*'s occupied by a molecule of component k. The symbols R and T have their usual meaning.

The temperature and concentration dependence of the interaction function g may assume various forms, depending on the molecular model used for its definition[6,14]. For instance, the incorporation of Huggins' orientational entropy contributions to ΔG[15] represents one particular example, application of which to polymer blends has been discussed by Koningsveld and Stepto[16]. We here represent all those different expressions in the form of a quadratic polynomial in φ_2, the coefficients of which will have different meanings for the different models. Thus,

$$g(T,\varphi_2) = g_0 + g_1\varphi_2 + g_2\varphi_2^2 \qquad (2)$$

Spinodal condition and liquid-liquid critical state are defined by[17-19]:

Spinodal:

$$L_1 + L_2 - 2g_0 + 2g_1(1 - 3\varphi_2) + 6g_2\varphi_2(1 - 2\varphi_2) = 0 \qquad (3)$$

Consolute state:

$$Q_1 - Q_2 - 6g_1 - 6g_2(1 - 4\varphi_2) = 0 \qquad (4)$$

where $L_k = 1/(m_k\varphi_k)$ and $Q_k = 1/(m_k\varphi_k^2)$.

Experimental cloud points in practically-binary mixtures of polyisoprene and polystyrene are collected in Fig. 1. The samples are of relatively low molar mass, in the range of which the chain lengths play an obviously dominant role, determining not only the widely varying location of critical temperatures, but also influencing the shape of the *cpc*. The bimodality of the miscibility gap in the 2.7/2.1 system changes into a shoulder in the 2.7/2.7 mixture, and has vanished altogether in the 0.82/2.1 blend. The 2.0/2.7 data by other workers do not seem to be consistent at all with the other three sets.

It has been shown previously that the *cpc*'s of Fig. 1 cannot be described with the *FHS* expression in its original form with g independent of concentration (then $g \equiv \chi$), and that the unusual, bimodal shape can be reproduced qualitatively if Eq. 2 is employed[21]. Here we extend the analysis somewhat further, assuming g_1 and g_2 to be independent of T, and the temperature dependence of g_0 to be given by the usual form

$$g_0 = g_{0s} + g_{0h}/T \qquad (5)$$

where g_{0s} and g_{0h} are constants. The enthalpic term g_{0h} should be of the order of 10^2 K in order to be acceptable within the model (nonpolar or weakly polar Van der Waals interactions).

Within the present scope we may identify the extrema of the *cpc*'s with critical points, and use those of the 2.7/2.1 system to determine g_1 and g_2 with Eq. 4. The *BVU* may be treated as a *mass* unit, arbitrarily set at 100g/mol, so that the relative chain lengths m_k are obtained by dividing molar mass by 100, and the φ's represent mass fractions. Critical points are located on the spinodal, hence Eq. 3 can be used to calculate g_0 and its temperature dependence. The g_{0h} value found on this basis with the measured coordinates of the two maxima is 5131 K, too large a value to be acceptable. Keeping the two concentrations fixed at the measured values, one would have to shift the critical temperatures to 120°C and 150°C, respectively, to bring g_{0h} down to 292 K. Obviously, such a manoeuvre is not justified by the data, and we might look for an better $g(T,\varphi_2)$ function. Alternatively, however, we may not strive for a fully quantitative reproduction of the data, and check whether Eqs 1, 2 and 5 are capable of covering the sensitivity of location and shape of the *cpc* toward chain length in a general sense.

Some trial and error analysis of the data from ref. 20 yields a set of parameters producing Fig. 2 which is in *qualitative* accordance with the data. In view of

the latters' large T-range, Eq. (5) was found not to be quite adequate and had to be replaced by the better approximation[22,23)]

$$g = g_{0s} + g_{0h}/T + g_{0k}T \qquad (5a)$$

where g_{0k} is a constant. The analysis shows that the extended *FHS* expression (Eqs 1, 2 and 5a) correctly predicts bimodality to appear at a given set of chain lengths, to vanish or change into a shoulder when chain length is varied. Miscibility gaps in blends showing shoulders and, occasionally, a bimodal shape, have not infrequently been reported. The present analysis indicates that such phenomena should not too readily be discarded or attributed to experimental errors, and may point to a marked dependence of χ on concentration..

The obtained description contains the above mentioned subtle features at the cost of the concentrations of the extrema that are too low, except for the right-hand maximum in system 2.7/2.1 and the shoulder in 2.7/2.7. The intersection of the two *cpc* branches in 2.7/2.1 indicates the occurrence of a (binary) nonvariant equilibrium between the three phases α, β and γ, in the experiment at about 126.5 0C, in the calculation at 127.3°C. The connection of the extensions of the binodals beyond the three-phase line $\alpha\beta\gamma$ are illustrated in detail in Fig. 2a, and.have been discussed extensively in a previous paper[5)].

The *cpc* of the 2.0/2.7 system, reported by other workers[20)], can now be predicted which results in a *cpc* that is located about 100^0C higher than the experimental data. This discrepancy illustrates an important hazard of studies in polymer blend thermodynamics. In the first place, the extreme sensitivity of the location to relatively small differences in chain length might suggest errors in the determination of molar masses to be behind the discrepancy. However, at the level of a few thousand g/mol such errors cannot reasonably be expected to have been all that large.

Other experimental problems suggest more obvious reasons For instance, the polyisoprene samples may have differed in *cis/trans* configuration, and steric configurations have been found to markedly influence the temperature location of blend miscibility gaps [24)]. This may well be the reason why, for instance, miscibility data of various authors on the system poly(vinyl methyl ether)/polystyrene cannot possibly be reconciled[25)]. It is further known that in research of this nature the purity of the constituents is critical[26,27)], traces of admixtures already being potentially detremental for a meaningful comparison of data.

Quasi-binary blends

The above example illustrates some of the difficulties encountered in the study of practically-binary systems. Non-negligible molar-mass distributions in the polymers cause additional problems. We may use a hypothetical system to analyse the situation, thus having precise *a priori* knowledge of the two *mmd*'s as well as the interaction function, and so investigate the significance of

conceivable evaluation methods for the latter. We use *FHS* systems without concentration dependence of the interaction parameter, giving the latter some attention in passing. There is no loss of generality involved since, if determination of the temperature dependence of χ already calls for extensive efforts, the usual concentration dependence can only be expected to further complicate the issue.

The appropriate ΔG function is identical in form to Eq 1, except for the definitions of Ω_k and φ_k which now read[12,17-19)]

$$\Omega_k = \Sigma(\varphi_{ki}/m_{ki})ln\varphi_{ki};\ \ \varphi_k = \Sigma\varphi_{ki} \qquad (6)$$

where *i* is the running index for the components within constituent k. The definitions of L_k and Q_k also change and become

$$L_k = 1/(m_{wk}\varphi_k);\ \ Q_k = \xi_{wk}/(m_{wk}\varphi_k^2) \qquad (6a)$$

where $\xi_{wk} = m_{zk}/m_{wk}$, and m_{wk} and m_{zk} are the weight- and z- average *BVU*-numbers of polymer constituent k, respectively.

We define each of the *mmd*'s of the polymers as the sum of two Schulz-Zimm (*SZ*) distributions, constructed so as to conform to chosen m_n, m_w and m_z values (m_{nk} is the number-average number of *BVU*'s occupied by polymer molecules k; $\xi_{nk} = m_{wk}/m_{nk}$). Setting $m_{w1} = 100$, $\xi_{n1} = 2$, $\xi_{w1} = 1.75$, and $m_{w2} = 500$, $\xi_{n2} = 3$, $\xi_{w2} = 2$, the construction procedure[30)] leads to the distribution parameter sets given in Table 1.The weight fractions of the two *SZ* functions a and b for polymer k are w_{ak} and w_{bk}, their m_w values m_{wak} and m_{wbk}. The ξ_n and ξ_w of the part distributions have each been taken identical in the two polymers. The continuous curve in Fig. 3 represents the so-constructed distribution curve for polymer 1. Other possible representations, all at the same m_w, ξ_n and ξ_w, are shown in Fig. 3 and Table 1. They refer to binary, arbitrary quaternary, and 'bell-shaped' quaternary distributions. The concentrations of the two added components to form the six-component 'bell-shaped' set in Table 1 do not show up on the scale of drawing. The other distributions discussed below exhibit quite analogous patterns.

Letting $g_{0s} = 0.05$, $g_{0h} = -15$ K, $g_1 = 0$, $g_2 = 0$, we define the system to exhibit lower-critical-solution behaviour, and g to be independent of concentration. Procedures described elsewhere[21,28-36)](also those used for Fig. 2) allow calculation of cloud points in terms of T against φ_2, the volume fraction of the second polydisperse polymer. The result is shown in Fig. 4 (set I, filled circles) for two *SZ* distribitions in each of the two polymers.

We now consider these calculated cloud points as experimental data and proceed to test the significance of various procedures for extracting interaction-parameter values from them. The simplest analysis involves complete neglect of the *mmd*'s. The system is thus treated as if it were strictly-binary and the extremum of the *cpc* (now regarded as a binodal) is identified with the critical point. Setting $m_1 = 100$ and $m_2 = 500$, we find $g_{0c} = 0.01047$ and $\varphi_{2c} = 0.309$

with Eqs 3 and 4, the latter value clearly not being in agreement with the location of the minimum in set I, which occurs at $\varphi_2 = 0.25$. Ignoring this deviation we estimate the critical temperature at 105.8°C and use it as one calibration point for $g_0(T)$ (Eq. 5). The other piece of information we might draw, for instance, from the two concentrations at 112.5°C (0.005 and 0.545) and, using calculation procedures for coexisting-phase compositions[21,28-36], find them not to coexist and, hence, to yield two different values for g_0. Using the average of these two values to be representative for 112.5°C, we obtain $g_{0s} = 0.098038$, $g_{0h} = -33.183$ K with Eqs 3 and 4, and calculate the lower drawn curve in Fig. 4. The deviations between the curve and the simulated data points (set I) are relatively large (4°C at $\varphi_2 = 0.6$, at a total temperature range of the cloud points of about 7°C for $0.05 \leq \varphi_2 \leq 0.6$), and so is the difference between the chosen and recovered values of g_{0s} and g_{0h}.

Whether or not one would accept such a data description, it has no value unless it allows correct prediction of data not used in obtaining the description, or data yet unknown. Therefore, we simulate another set of cloud points in the same manner as set I, but for $m_{w2} = 100$, the other characteristics being kept the same (set II). A binary prediction on the basis of the g_{0s} and g_{0h} values obtained above, yields the upper drawn curve in Fig. 4 which is very far from the truth.

In a practical situation the thermodynamics of the system are not known *a priori*, and one might be inclined to blame the discrepancy on a possible concentration-dependence of g. Setting $g = g_0 + g_1\varphi_2$, with both coefficients depending on T, and using an appropiately adapted calculation procedure[21,28-36], we find the parameter values given in Table 2. The description of set I has improved greatly, at least at $\varphi_2 < 0.6$, and would probably be considered satisfactory if no other data were available (lower dashed curve in Fig. 4). However, if they are (set II), we note that the prediction has hardly improved (upper dashed curve). Evidently, neglect of the *mmd*'s cannot lead to meaningful values of the interaction parameters, a conclusion that could not be drawn on the basis of set I alone. Neither can be concluded too easily that a concentration dependence of χ prevails.

If the *mmd*'s are included there are two cloud-point concentrations at a given T that do not represent conjugate phases[1-3], but the g_0 values so obtained can still be calibrated against T, for instance with the cloud points of set I. If the *mmd*'s of the simulation itself were used, one obviously would then recover $g_{0s} = 0.05$, $g_{0h} = -15$ K, the values chosen originally. However, we usually do not know the *mmd*'s all that accurately and might tend to use binary approximations (w_{k1},m_{k1}; w_{k2},m_{k2}; w_{ki} being the weight fraction of component *i* in polymer k, *i* = 1,2)) that have at least the virtue of being unambiguously determined by m_w, ξ_n, and ξ_w[30]. A quite acceptable description of set I is obtained (Fig. 5, lower dashed curve) but g_{0s} and g_{0h} still deviate greatly from the chosen values and, accordingly, the prediction of set II is poor (Fig. 5, curve 1).

Knowing the 'correct' g_{0s} and g_{0h} values, we realize that the reason for the discrepancy must be sought in the approximation of the *mmd*'s. Sets of four components in each of the polymers yield a description of set I that can hardly be distinguished from that obtained with the binary *mmd*'s (Fig. 5, lower dashed curve). The prediction of set II, however, is about 45^0C too low and demonstrates that the $g_0(T)$ function is still too far off (Fig. 5, curve 2; Table 2).

In the above example the four weight fractions of the individual components within a constituent polymer were calculated quite arbitrarily, and do not reflect the bell shape of the continuous distributions used for the simlulation of cloud points (see Table 1 and Fig. 3). We may adapt the sets of four components so that they come a little closer to the bell shape (at the chosen m_w, ξ_n and ξ_w values, Fig.3) The effect is surprising, the gap between simulated and predicted set II being reduced by about 50% (Fig. 5, curve 3). Also the interaction function derived from the cloud points of set I comes considerably closer to the chosen one (Table 2). Adding minute amounts (not enough to show up in Fig. 3) of two more components at both ends of the *mmd*'s, retaining the rough resemblance of the bell shape, we obtain considerable further improvement, the average difference between set II and its prediction being only about 3^0C (Fig. 5, curve 4). The g_{0s} and g_{0h} values are now very close to those set in the example (Table 2) and the description of set I is excellent (lower drawn curve).

This numerical exercise indicates that the extraction of significant interaction parameter values from cloud points is no trivial matter and calls for quite accurate information about the *mmd*'s involved, probably more accurate than is usually available. Moreover, the inclusion of additional data, like set II in the example, appears to be essential for a reliable anchoring of the $g_0(T)$ function. To decide whether all this is sufficient we would need still one more additional set of data which we obtain as before, simulating set III for $m_{w1} = m_{w2} = 500$ and retaining the other distribution characteristics. The constants g_{0s} and g_{0h} found by fitting of the combined sets I and II are listed in Table 2 for binary and six-component (bell shaped) *mmd*'s. Figure 6 shows that, again, the binary *mmd* representation does not suffice (dashed curves), and that the six-component bell-shaped *mmd*'s yield the required result, both in description of sets I and II, and prediction of set III (drawn curves).

The extra data do not need to be cloud points. Measurements could be limited to a single blend, if the cloud points are then supplemented by spinodal points obtained with scattering methods. Spinodal points can be simulated easily with Eq. 3, some are shown in Fig. 6 for set I. Fitting $g_0(T)$ to cloud points and spinodal points for set I alone yields quite acceptable predictions for sets II and III, in spite of the considerable temperature extrapolations involved (Fig. 6, dash-dot curves). The inclusion of spinodal data being so obviously beneficial may be due to the fact that scattering methods 'measure' the second derivative of ΔG with respect to concentration whereas cloud points are determined by chemical potentials, *i.e.*, the first derivative. Also, within the *FHS* framework,

the spinodal does not depend on details of the *mmd*'s, as cloud points do, but merely on the two m_w's (Eq. 6a).

Melting-point depression

Melting-point depressions in a partially-crystalline polymer blend might be expected to supply an alternative extra source of information. If the second polymer is the crystallizable constituent we may write for a binary *FHS* blend)[13)]

$$(\Delta H_{f,u}/R)(1/T_{m2}^{0} - 1/T) = (ln\varphi_2)/m_2 + (1/m_2 - 1/m_1)\varphi_1 + (g_{0s} + g_{0h}/T)\varphi_1^{2} \quad (7)$$

where $\Delta H_{f,u}$ is the molar heat of fusion per mol of crystallizable repeat units in polymer 2; T_{m2}^{0} and T are the equilibrium melting points of polymer 2 in its pure state and in the blend, respectively. Figure 7 shows some solubility curves for polymer 2 (melting point against volume fraction), calculated with Eq. 7 for $m_1 = 100$, $m_2 = 100$, $\Delta H_{f,u} = 1000$ cal/mol, $T_{m2}^{0} = 400$ K. Three possible two-phase states of the liquid mixture are considered and described as in the preceding section with three sets (g_{0s}/g_{0h}) representing lower-critical miscibility above 425 K, and upper-critical miscibility below 375 K and below 405 K (Table 3).

If the liquid/liquid critical point is close to T_{m2}^{0} (system 2) the melting-point depressions are very small in the full composition range and, since miscibility gap and solubility curve interfere, there is a nonvariant three-phase equilibrium ($\alpha/\beta/\gamma$)[1)]. The solubility curve must assume a sigmoid shape in order to pass through points α and β that represent the two liquid phases on the three-phase line $\alpha\beta\gamma$ at 399.6 K. The spinodal passes through maximum and minimum of the very shallow metastable solubility curve[37)].

The experimental determination of equilibrium melting points in polymers is extremely difficult and a reduction of the probable error to ± 1 K would call for exceptionally good work indeed. Even then, the error bar on the solubility curves is too large to allow distinction between the three types of demixing, and reliable determination of parameters like g_{0s} and g_{0h} is out of the question. Even complete miscibility in the liquid state ($g_{0s} = 0$, $g_{0h} = 0$) cannot be distinguished reliably. The only type of blends in which the melting-point depression might give an indication of the. magnitude of the interaction parameter are those in which very strong specific interactions are operative (see solubility curve for $g_{0s} = 0$, $g_{0h} = -50$ K). The average χ value is - 0.13 at $370 < T < 400$ whereas it amounts to only + 0.02 for critical miscibility

It is remarkable that experimental melting points cannot distinguish at all between such widely varying cases of demixing like 1 and 3, the latter referring to metastable demixing of the liquid state. Within the present examples a rough distinction can only be made between complete miscibility (4) and border-case 2 at $\varphi_2 < 0.5$, but this is useless in the present context.

These results do not depend on the parameter values chosen here and must be regarded to have general validity.

Discussion

The present analysis demonstrates that

(*a*) cloud-point data on a single blend cannot produce significant information on the interaction parameter and its dependence on temperature and concentration;

(*b*) two, or better three sets of cloud points for different molar-mass distributions are needed to obtain $\chi(T,\varphi_2)$ with confidence;

(*c*) a single blend may still supply useful information provided the cloud points are supported by additional data of a different nature, for example, spinodal points;

(*d*) neglect of the two molar-mass distributions leads to meaningless data on $\chi(T,\varphi_2)$;

(*e*) melting-point depressions do not supply significant information on the interaction parameter.

These conclusions refer to model data, not affected by experimental errors. In an actual experimental situation such unavoidable errors will further detract from the significance of blend χ parameter values. Moreover, a comparison with the aid of the thermodynamic model obeyed by the system, as available here, is not possible in experimental practice. Finally, the attainment of equilibrium is usually much retarded in polymer blends, which introduces another source of inaccuracy. Interaction parameter values on blends, as reported in the literature, should therefore be carefully scrutinized as to the way in which they have been obtained

Acknowledgement

The authors are indebted to professor Walter H. Stockmayer (Dartmouth College, Hanover, N.H.) for stimulating discussions.

References

1. Schreinemakers, F.A.H. in: Bakhuis Roozeboom, H.W. "*Die heterogenen Gleichgewichte vom Standpunkte der Phasenlehre*", Vol. III, Part 2, Vieweg, Braunschweig, **1913**
2. Tompa. H., *Trans.Farad.Soc.* **1949**, *45*, 1142
3. Koningsveld, R., Staverman, A.J., *J.Polym.Sci.* **1967**, *C16*, 1775
4. Wolf, B.A., *Adv.Polym.Sci.* **1972**, *10*, 109
5. Šolc, K., Koningsveld, R., *J.Phys.Chem.* **1992**, *96*, 4056
6. Koningsveld, R. *Macromol.Symp.* **1994**, *78*, 1
7. Staverman, A.J., Van Santen, J.H., *RecTrav.Chim.Pays-Bas* **1941**, *60*, 76
8. Staverman, A.J., *Rec.Trav.Chim.Pays-Bas* **1941**, *60*, 640
9. Huggins, M.L., *J.Chem.Phys.* **1941**, *9*, 440
10. Huggins, M.L., *Ann.N.Y.Acad.Sci.* **1942**, *43*, 1
11. Flory, P.J., *J.Chem.Phys.* **1941**, *9*, 660
12. Flory, P.J., *J.Chem.Phys.* **1942**, *10*, 51; **1944**, *12*, 425
13. Flory, P.J., "Principles of Polymer Chemistry", Cornell Univ.Pr., Ithaca
14. Schäfer-Soenen, H., Moerkerke, R., Berghmans, H., Koningsveld, R., Dušek, K, Šolc, K., *Macromolecules* **1997**, *30*, 410
15. Huggins, M.L., *J.Phys.Chem.* **1970**, *74*, 371; **1976**, *80*, 1317
16. Koningsveld, R., Stepto, R.F.T., *Macromolecules* **1977**, *10*, 1166
17. Stockmayer, W.H., *J.Chem.Phys.* **1949**, *17*, 588
18. Tompa, H., "*Polymer Solutions*", Butterworth, London **1956**
19. Koningsveld, R., *Disc.Farad.Soc.* **1970**, *No.49*, 145
20. McIntyre, D., Rounds, N., Campos-Lopez, E., *ACS Polym.Prepr.* **1969**, *10*, 531
21. Koningsveld, R. Kleintjens, L.A., Schoffeleers, H.M., *Pure Appl. Chem* **1974**, *39*, 1
22. Delmas, G., Patterson, D., Somcynski, T., *J.Polym.Sci.* **1962**, *57*, 59
23. Van Opstal, L., Koningsveld, R., *Polymer*, **1992**, *33*, 3433, 3445
24. Beaucage, G., Stein, R.S., Koningsveld, R., *Macromolecules* **1993**, *26*, 1603
25. Ongoing work, Univ.Leuven, Belgium, Laboratory for Polymer Reasearch
26. Wolf, B.A. and Geerissen, H., *Colloid Polym.Sci.* **1981**, *259*, 1214
27. Gordon, M., personal communication 1988; also ref. 23, p. 3435
28. Šolc, K., *Macromolecules* **1970**, *3*, 665
29. Šolc, K., *Macromolecules* **1986**, *19*, 1166
30. Koningsveld, R., Šolc, K., *Collect.Czech Chem.Comm.* **1993**, *58*, 2305
31. Šolc,. K., *Macromol.Symp.* **1993**, *70/71*, 93

32. Koningsveld, R., Šolc, K., MacKnight, W.J., *Macromolecules* **1993**, *26*, 6676
33. Mumby, S.J., Sher, P., Eichinger, B.E., *Polymer* **1993**, *34*, 2540
34. Vanhee, S., Kiepen, F., Brinkmann, D., Borchard, W., Koningsveld, R., Berghmans, H., *Macromol.Chem.Phys.* **1994**, *195*, 759
35. Šolc, K., Koningsveld, R., *Collect.Czech Chem.Commun.* **1995**, *60*, 1689
36. Mumby, S.J., Sher, P., Van Ruiten, J., *Polymer* **1995**, *36*, 2921
37. Koningsveld, R., Stockmayer, W.H., Nies, E., "*Polymer Phase Diagrams*", Oxford Univ.Pr., in preparation

Captions to figures

Fig.1. Cloud points in practically-binary mixtures of anionic polyisoprene (PI) and anionic polystyrene (PS) for indicated values of the number-average molar mass in kg/mol. Data taken from two sources: ref. 20, 2/2.7; ref. 21, 2.7/2.7, 2.7/2.1 and 0.82/2.1. Weight faction of PS: w_2.

Fig.2. Phase diagram calculated with Eqs 1, 2 and 5a for indicated sets of m_1/m_2 values. Heavy curves: binodals, light curves: spinodals; critical points: o; three-liquid-phase equilibrium: ▲—▲—▲. Interaction-parameter values: $g_{0s} = -0.42757$, $g_{0h} = 162.32$ K, $g_1 = -0.1$, $g_2 = 0.091$..

Fig.2a. Details of the equilibrium curves around three-phase equilibrium $\alpha\beta\gamma$ in Fig 2 ($m_1 = 27$, $m_2 = 21$). Heavy drawn curves: stable equilibrium, dashed curves: metastable and unstable equilibrium. Light drawn curve: spinodal; critical points: o.

Fig. 3. Possible molar-mass distributions for polymer 1 ($m_w = 100$, $\xi_n = 2$, $\xi_w = 1.75$). Curve: sum of two *SZ* distributions; heavy drawn lines: binary polymer distribution; heavy dashed lines: arbitrary quaternary distribution; light drawn lines: 'bell-shaped' quaternary distribution (Table 1)

Fig. 4. Cloud points (●) for two hypothetical polymer blends (sets I and II), calculated with Eqs 1 and 5 for $g_{0s} = + 0.05$, $g_{0h} = - 15$ K, $g_1 = 0$, $g_2 = 0$. Polymer *mmd*s represented by a sum of two *SZ* functions. Critical points: o. Curves: strictly-binary reproductions of cloud points with estimated values of g_{0s} and g_{0h}. Lower drawn curve: $g_1 = 0$, $g_2 = 0$; lower dashed curve: $g_1 \neq 0$, $g_2 = 0$; upper drawn and dashed curves: corresponding predictions of set II (see text)

Fig. 5. Cloud-point data of Fig. 4. Lower dashed curve: representation of set I by two binary polymers and by two quaternary polymers. Lower drawn curve: two six-component polymers. Curves 1-4: predictions of set II with increasingly accurate approximations of the polymers' *mmd*'s. Critical points: o.

Fig.6. Cloud points (●) and spinodal points (▲) for three polymer blends (sets I, II and III). Interaction paramerters obtained from cloud-point sets I and II. Dashed curves: description of sets I and II, and prediction of set III on the basis of binary polymer distributions; drawn curves: ditto with six-component *mmd*'s. Dash-dot curves: parameters obtained from cloud-point and spinodal data on set I: description of set I and prediction of sets II and III. Critical points: o.

Fig.7. Solubility curves and miscibility gaps (heavy curves) calculated with Eqs 1, 3-5, 7 for $\Delta H_{f,u} = 1000$ cal/mol, $T_{m2}^0 = 400$ K., $m_1 = 100$, $m_2 = 100$, and various interaction-parameter values (Table 3). Three-phase-equilibrium: ▲—▲—▲; light curves: spinodals; dashed curves: metastable equilibria; error bar for ± 1 K: ⌶; critical points: o.

Table 1

Molar-mass distribution characteristics for set I

Polymer 1	Polymer 2
$m_w = 100$	$m_w = 500$
$\xi_n = 2$	$\xi_n = 3$
$\xi_w = 1.75$	$\xi_w = 2$

Sum of 2 Schulz-Zimm distributions ($\xi_{na} = \xi_{nb} = 1.5$; $\xi_{wa} = \xi_{wb} = 4/3$)

$w_{a1} = 0.3909$; $m_{wa1} = 55.22$	$w_{a2} = 0.5$; $m_{wa2} = 146.4$
$w_{b1} = 0.6091$; $m_{wb1} = 169.8$	$w_{b2} = 0.5$; $m_{wb2} = 853.6$

Binary polymers

$w_{11} = 0.6387$; $m_{11} = 34.86$	$w_{12} = 0.6213$; $m_{12} = 109.6$
$w_{21} = 0.3613$; $m_{21} = 215.1$	$w_{22} = 0.3787$; $m_{22} = 1140$

Four-component polymers

Arbitrary

$w_{11} = 0.3046$; $m_{11} = 23.34$	$w_{12} = 0.25$; $m_{12} = 61.90$
$w_{21} = 0.3046$; $m_{21} = 87.10$	$w_{22} = 0.25$; $m_{22} = 231.0$
$w_{31} = 0.1954$; $m_{31} = 71.76$	$w_{32} = 0.25$; $m_{32} = 360.8$
$w_{41} = 0.1954$; $m_{41} = 267.8$	$w_{42} = 0.25$; $m_{42} = 1346$

'Bell-shaped'

$w_{11} = 0.0766$; $m_{11} = 10$	$w_{12} = 0.3043$; $m_{12} = 75$
$w_{21} = 0.4405$; $m_{21} = 50$	$w_{22} = 0.3135$; $m_{22} = 200$
$w_{31} = 0.4216$; $m_{31} = 125$	$w_{32} = 0.2816$; $m_{32} = 900$
$w_{41} = 0.0613$; $m_{41} = 400$	$w_{42} = 0.1006$; $m_{42} = 1600$

Six-component polymers

$w_{11} = 0.01$; $m_{11} = 5$	$w_{12} = 0.01$; $m_{12} = 50$
$w_{21} = 0.0553$; $m_{21} = 10$	$w_{22} = 0.2864$; $m_{22} = 75$
$w_{31} = 0.4408$; $m_{31} = 50$	$w_{32} = 0.3208$; $m_{32} = 200$
$w_{41} = 0.4407$; $m_{41} = 125$	$w_{42} = 0.2868$; $m_{42} = 900$
$w_{51} = 0.0482$; $m_{51} = 400$	$w_{52} = 0.0911$; $m_{52} = 1600$
$w_{61} = 0.005$: $m_{61} = 600$	$w_{62} = 0.005$: $m_{62} = 2000$

Table 2

Values of interaction parameters g_{0s} and g_{0h} from cloud points for various distributions

	g_{0s}	g_{0h}/K
Set I:		
2 *SZ* functions (model system)	0.05	- 15
Binary polymers	0.079091	- 26.033
Quaternary polymers (arbitrary)	0.066503	- 21.260
Quaternary polymers ('bell-shaped')	0.056757	- 17.555
Six-component polymers	0.048979	- 14.595
Sets I and II:		
Binary polymers	0.050833	- 15.043
Six-component polymers	0.050050	- 15.011
Set I and Spinodal:		
Binary polymers	0.079557	- 26.238
Six-component polymers	0.049188	- 14.683
Set I:		
single-component polymers	0.098038	- 33.183
single-component polymers ($g_1 \neq 0$)	0.11132	- 38.372
$g_1 = -0.04193 + 14.993/T$		

Table 3

Interaction-parameter values for Fig. 7

	T_c/K	g_{0s}	g_{0h}/K
System 1	425	0.15506	- 57.402
System 2	405	- 0.22839	100.60
System 3	375	- 0.09333	42.498
System 4	-	0	0
System 5	-	0	- 50

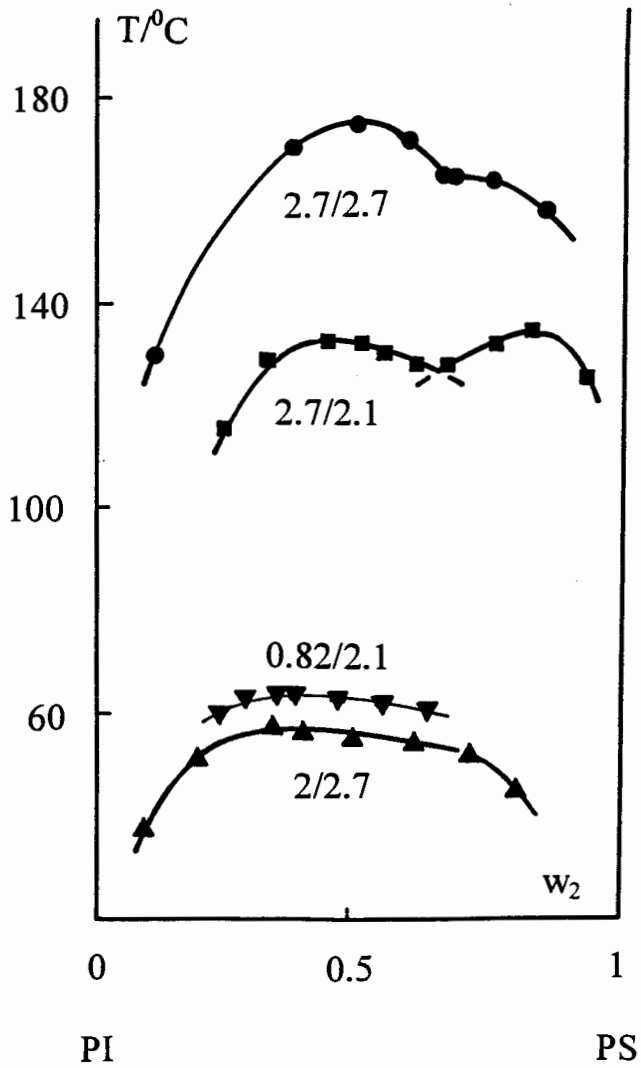
T/°C
180
140
100
60
2.7/2.7
2.7/2.1
0.82/2.1
2/2.7
w2
0
0.5
1
PI
PS

Fig. 1

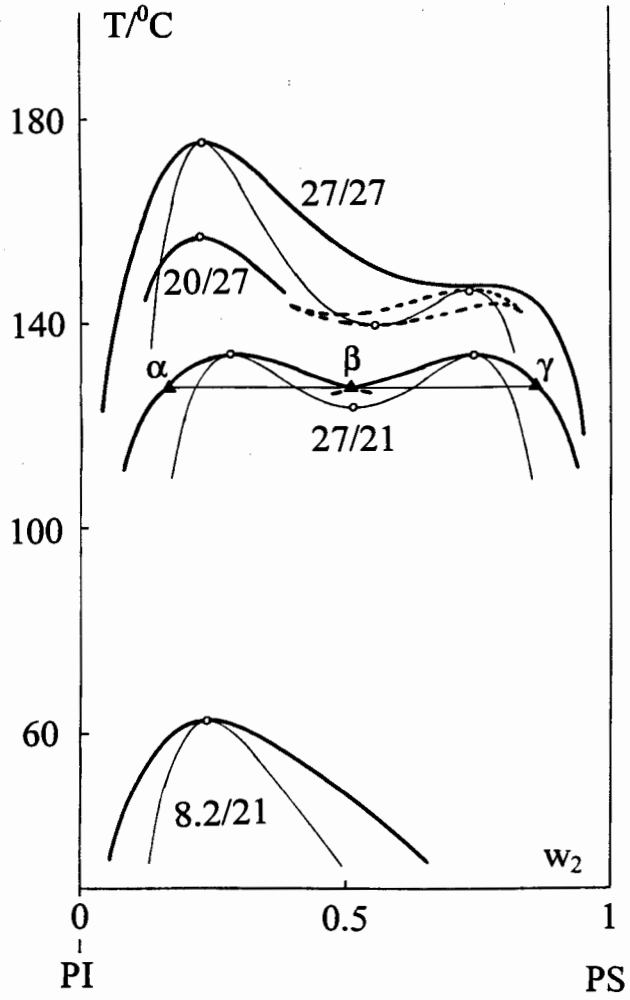
T/°C
180
140
100
60
27/27
20/27
α
β
γ
27/21
8.2/21
w2
0
0.5
1
PI
PS

Fig. 2

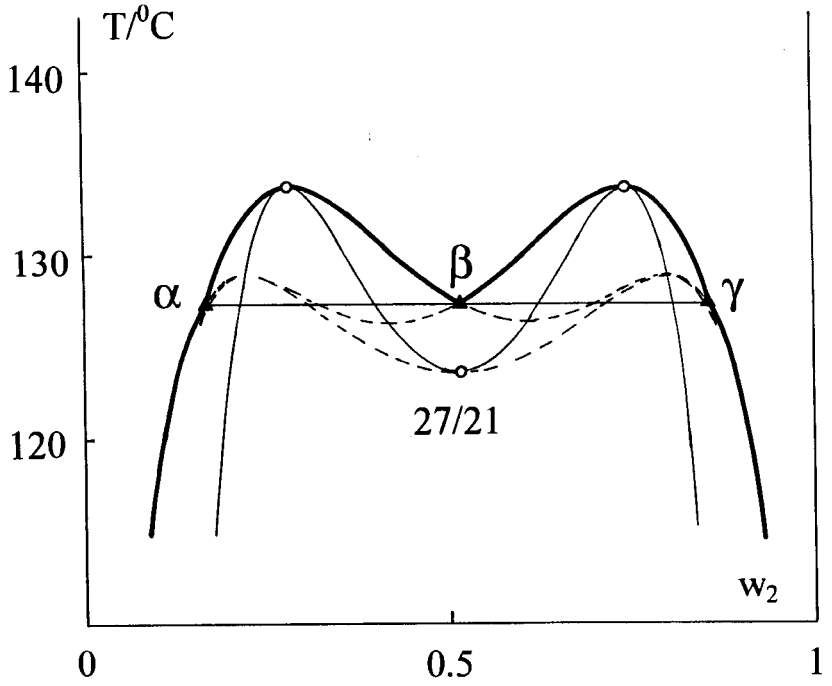
T/⁰C
140
130
120
α
β
γ
27/21
w2
0
0.5
1

Fig. 2a

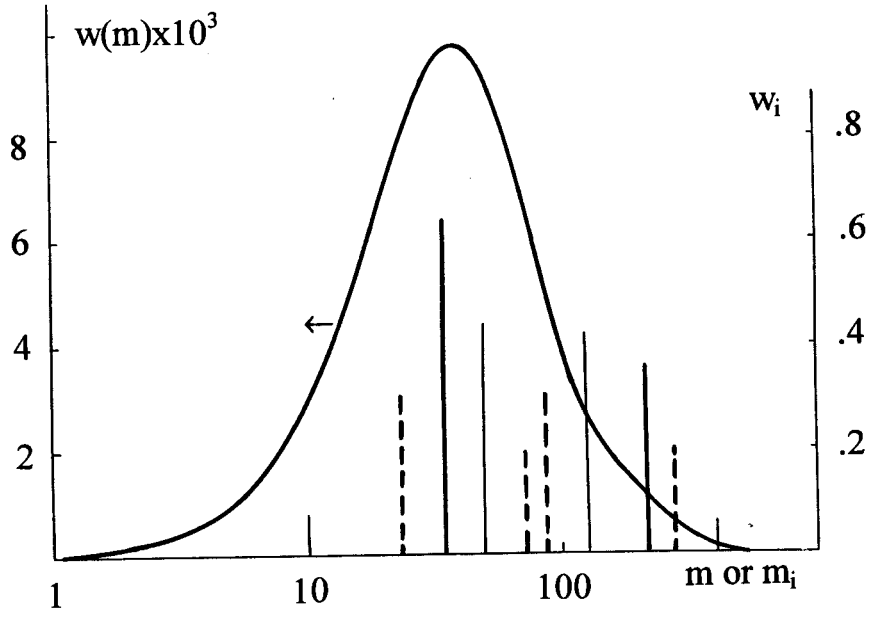
w(m)x10³
wi
8
6
4
2
.8
.6
.4
.2
1
10
100
m or mi

Fig. 3

Fig. 4.

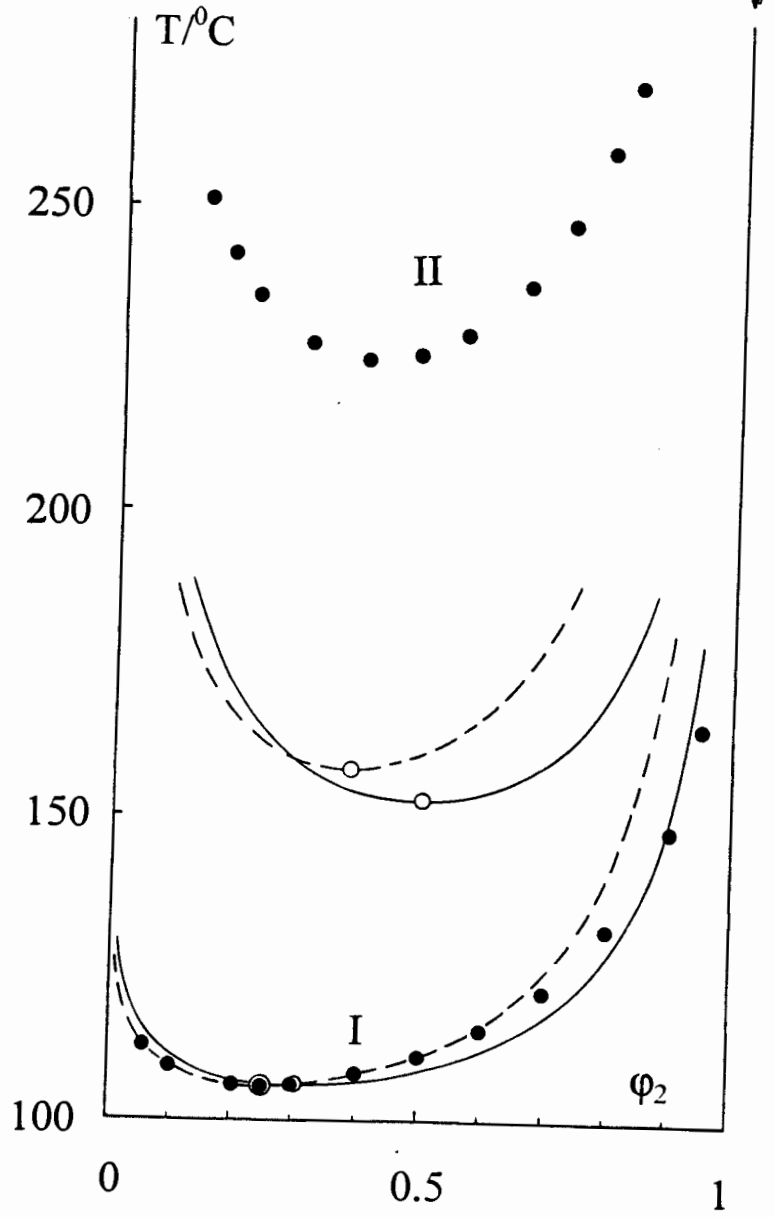
T/°C
250
200
150
100
II
I
φ2
0
0.5
1

Fig. 5.

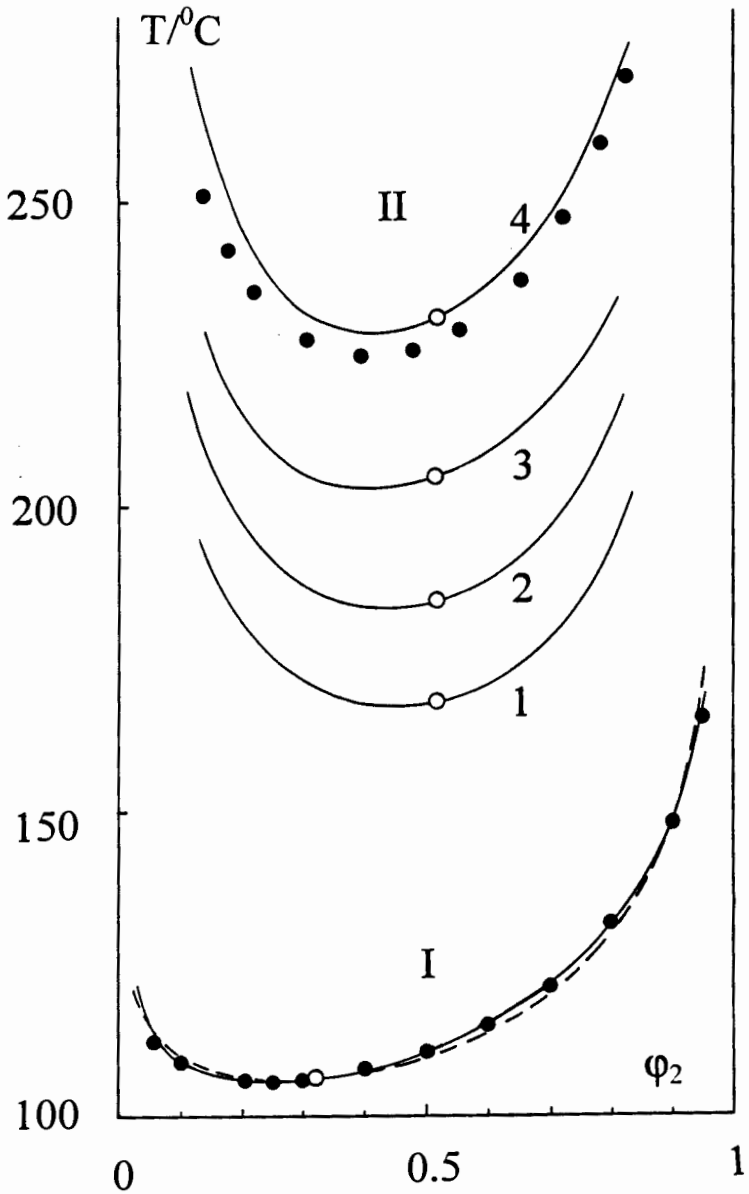
T/°C
250
200
150
100
II
4
3
2
1
I
φ2
0
0.5
1

Fig.6.

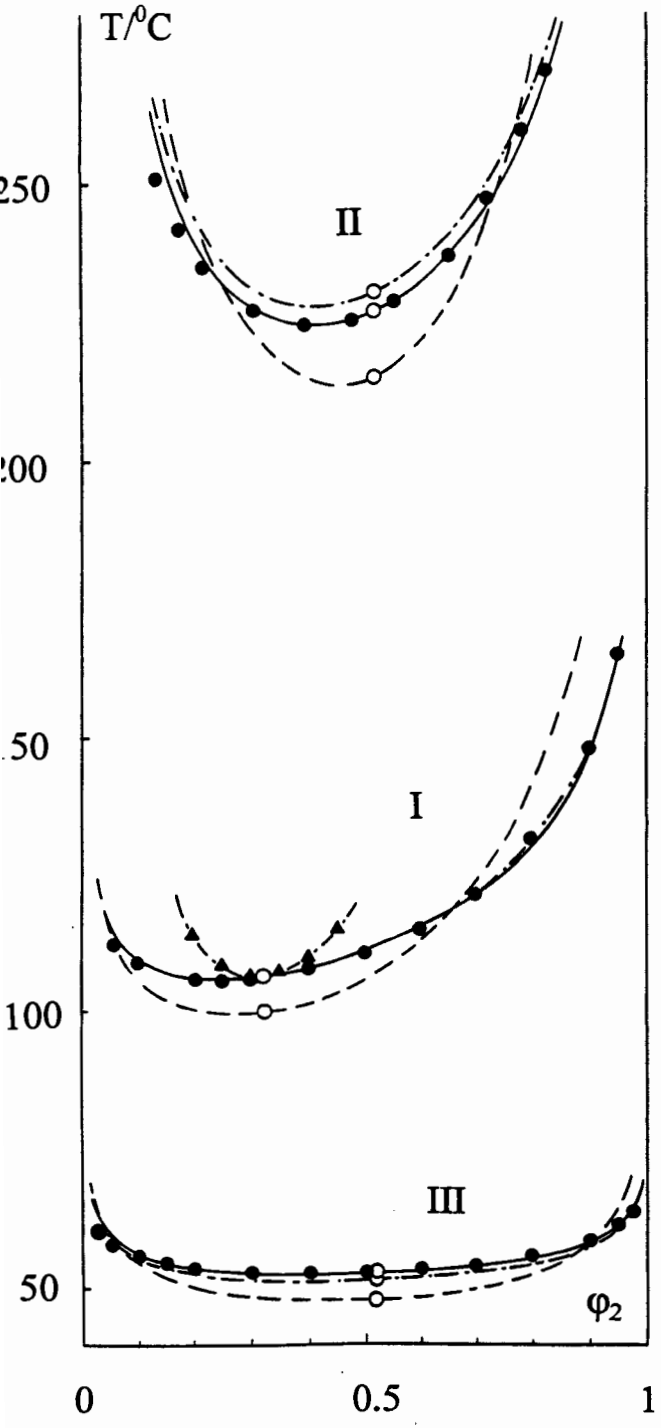
T/°C
250
200
150
100
50
II
I
III
φ2
0
0.5
1

Fig.7

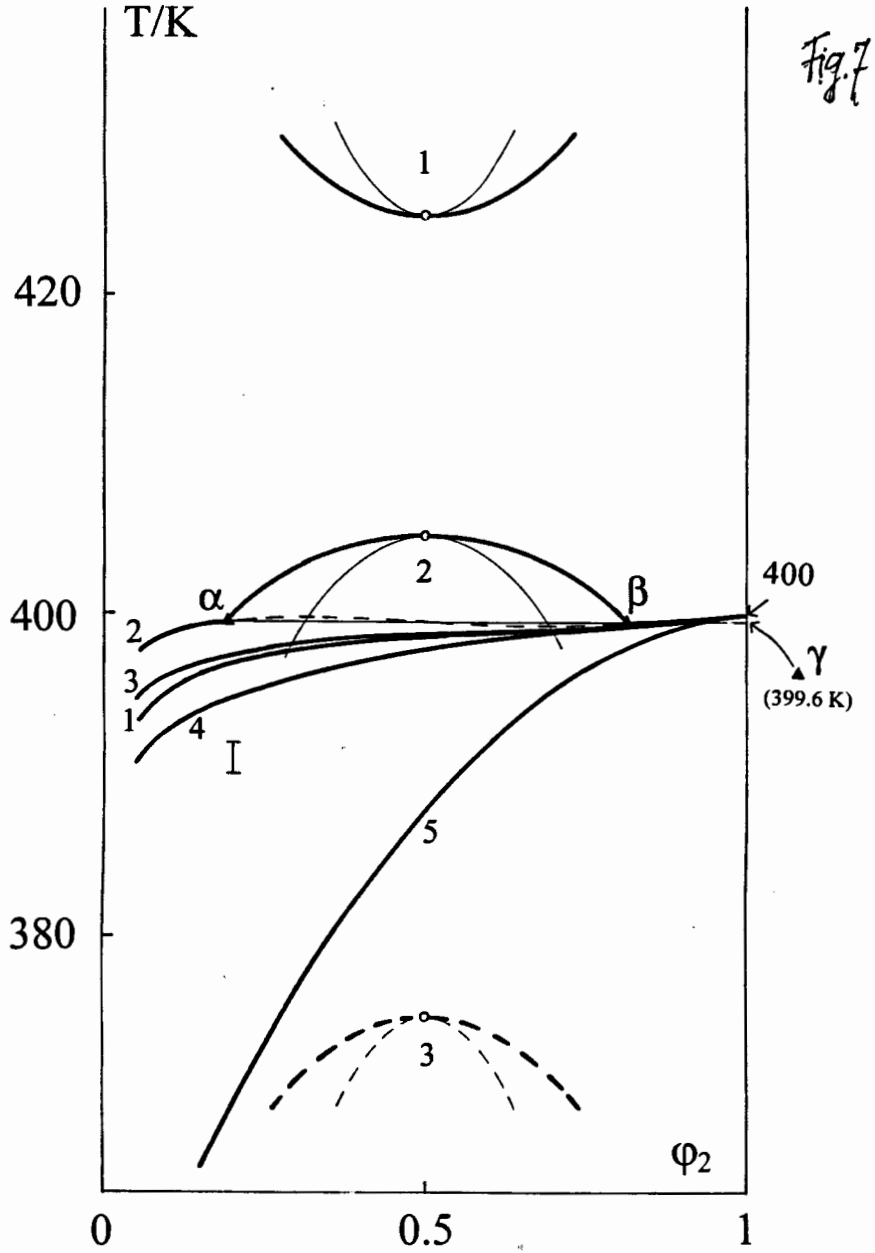
T/K
420
400
380
1
2
3
4
5
α
β
γ
400
(399.6 K)
I
φ2
0
0.5
1